RSC Advances

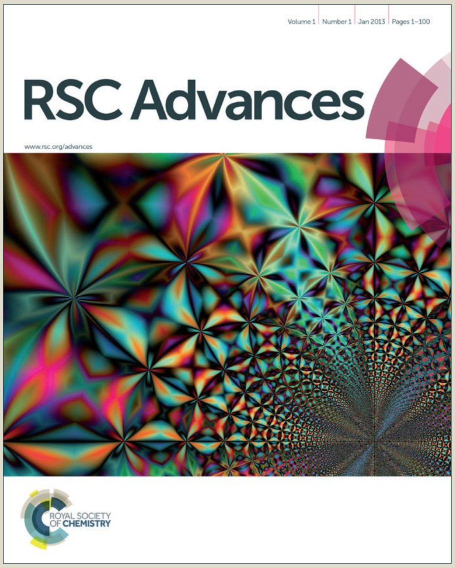

ROYAL SOCIETY OF CHEMISTRY

www.rsc.org/advances

Journal Name

ARTICLE

Butadiene dyes based on 3-(dicyanomethylidene)indan-1-one and 1,3-bis(dicyanomethylidene)indane: Synthesis, characterization and solvatochromic behaviour

Received 00th January 20xx,
Accepted 00th January 20xx

DOI: 10.1039/x0xx00000x

www.rsc.org/

Javier Francos,[a] Sergio E. García-Garrido,*[a] Javier Borge,[b] Francisco J. Suárez[a] and Victorio Cadierno*[a]

Novel donor-acceptor butadiene chromophores were synthesized by Knoevenagel condensation of different diaryl-substituted enals with 3-(dicyanomethylidene)indan-1-one and 1,3-bis(dicyanomethylidene)indane. The structures of two of these compounds were unambiguously confirmed by means of single-crystal X-ray diffraction. The absorption spectra of these dyes, as well as their solvatochromic behaviour, were studied in detail. In addition, DFT and TD-DFT quantum chemical calculations were performed to assess information regarding the topologies and absolute energies of their frontier molecular orbitals, as well as their absorption spectra.

Introduction

The design, synthesis and photophysical evaluation of organic π-conjugated systems has been deeply studied during the last decades due to the enormous potential of these materials for electronic, optoelectronic, and photonic applications.[1] Push-pull molecules, *i.e.* organic molecules end-capped with electron-donor (D) and electron-acceptor (A) units at the ends of a π-conjugated spacer, are representative examples of this class of compounds, whose properties lie in the intramolecular charge-transfer (ITC) between the donor and acceptor groups.[2] ITC provides the D-π-A systems with additional properties such as dipolar character, intense colour, crystallinity, and chemical and thermal robustness.

The indan-1,3-dione unit is one of the most common acceptor groups employed in the preparation of push-pull molecules (Fig. 1). Hundreds of such chromophores have been described in the literature, as well as applications thereof in diverse fields: nonlinear optics (NLO),[3] organic light-emitting diodes (OLEDs),[4] dye-sensitized solar cells (DSSCs),[5] organic photovoltaic cells (OPVs),[6] anion sensing and recognition,[7] or as photoinitiators in polymerization processes,[8] to name a few.

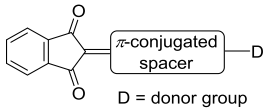

Fig. 1 Generic structure for push-pull molecules based on indan-1,3-dione.

In this context, we recently reported the preparation of a series of butadiene dyes **A** by dehydrative coupling of indan-1,3-dione with different diaryl-substituted terminal propargylic alcohols (Scheme 1).[9] The process involves the initial indium-catalyzed Meyer-Schuster rearrangement of the alkynol,[10,11] followed by the Knoevenagel condensation of the resulting enals with the 1,3-dicarbonyl compound. An evaluation of the optical properties of these species showed that they exhibit intense absorption bands in the visible region (405-565 nm), along with a pronounced solvatochromic behaviour.[9]

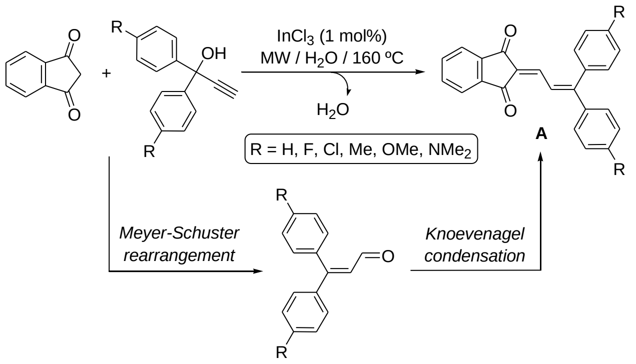

Scheme 1 Synthesis of butadiene dyes from indan-1,3-dione and terminal alkynols.

It is well-known that the electron withdrawing ability of the indan-1,3-dione unit can be enhanced by replacing one or both carbonyls by the dicyanomethylidene group.[12] This fact

---

[a] Laboratorio de Compuestos Organometálicos y Catálisis (Unidad Asociada al CSIC), Centro de Innovación en Química Avanzada (ORFEO-CINQA), Departamento de Química Orgánica e Inorgánica, Instituto Universitario de Química Organometálica "Enrique Moles", Facultad de Química, Universidad de Oviedo, Julián Clavería 8, E-33006 Oviedo, Spain. E-mail: garciagsergio@uniovi.es (S.E.G.-G.), vcm@uniovi.es (V.C.); Fax: +(34) 985103446; Tel.: +(34) 985103453.

[b] Departamento de Química Física y Analítica, Centro de Innovación en Química Avanzada (ORFEO-CINQA), Facultad de Química, Universidad de Oviedo, Julián Clavería 8, E-33006 Oviedo, Spain.

† Electronic Supplementary Information (ESI) available: Figures showing the optimized structures, cartesian coordinates and electronic energies for the computed species (*E*)-**4a**, (*Z*)-**4a**, **4f** and **5f**, a plot of λ_{max} (CH_2Cl_2 solution) *vs* Hammett coefficients for compounds **5a-f**, and a table giving melting point data for **4-5a-f**. CCDC 1442704 (**4d**) and 1442705 (**5b**). See DOI: 10.1039/x0xx00000x

prompted us to study the preparation, and evaluation of the optical properties, of related butadienic compounds containing 3-(dicyanomethylidene)indan-1-one **B** and 1,3-bis(dicyanomethylidene)indane **C** as the acceptor groups (Fig. 2). We would like to remark at this point that this type of 1,1-diaryl-substituted butadiene dyes have virtually no precedents in the literature.[13,14] The results from this study are presented herein.

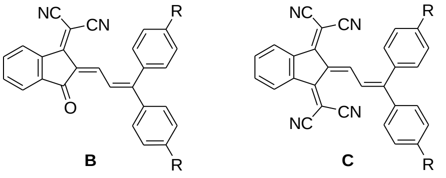

R = H, F, Cl, Me, OMe, NMe_2

Fig. 2 Structure of the butadiene dyes synthesized in this work.

Results and discussion

Initially, we attempted the preparation of the target butadienes by applying the methodology previously employed for the synthesis of the related indan-1,3-dione derivatives **A** (see Scheme 1), starting from the corresponding propargylic alcohols and 3-(dicyanomethylidene)indan-1-one (**2**), or 1,3-bis(dicyanomethylidene)indane (**3**). Disappointingly, under the same reaction conditions, mixtures of the desired compounds and butadienes **A**, resulting from the partial hydrolysis of the dicyanomethylidene moieties, were obtained. Fortunately, compounds **4-5a-f** could be selectively obtained (78-94% yield) through a classical Knoevenagel condensation of the corresponding enals **1a-f** with **2** and **3**, respectively, in a non-aqueous environment (Scheme 2). In the case of **4a-f**, the reaction took place smoothly in ethanol, at r.t., in the presence of catalytic amounts of morpholine. Although this procedure allows also the access to butadienes **5a-f**, much higher yields were in this case attained performing the Knoevenagel reaction in acetic anhydride at 60 °C (Scheme 2).

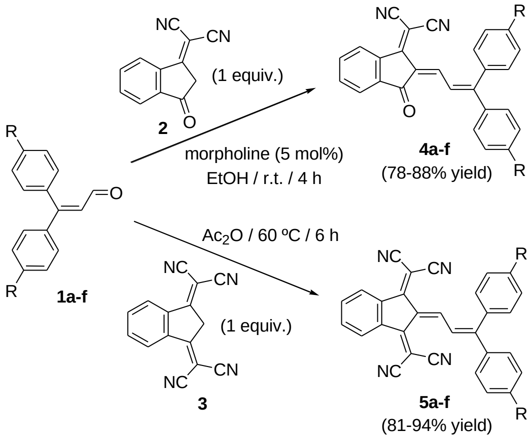

R = H (**a**), F (**b**), Cl (**c**), Me (**d**), OMe (**e**), NMe_2 (**f**)

Scheme 2 Synthesis of butadiene dyes **4a-f** and **5a-f**.

Characterization of compounds **4-5a-f** was achieved by means of standard spectroscopic techniques (HRMS, IR as well as multinuclear NMR) and elemental analyses, all data being fully consistent with the proposed formulations (details are given in the Experimental Section). In this regard, key spectroscopic features are the following: (*i*) (IR) the presence of characteristic absorption bands at 1686-1699 cm^{-1} and 2191-2234 cm^{-1} for the carbonyl and cyano groups, respectively; (*ii*) (^1H NMR) typical doublet signals ($^3J_{HH}$ = 11.4-12.6 Hz) for the olefinic protons of the butadiene chain, which resonate at *ca.* δ_H 8.40 and 8.80 ppm for **4a-f**, and 6.90 and 8.00 ppm for **5a-f**; (*iii*) ($^{13}C\{^1H\}$ NMR) characteristic singlet resonances for the C=O and C≡N carbons in the δ_c ranges 189.1-191.8 and 112.6-118.0 ppm, respectively.

Interestingly, the NMR spectra obtained for the 3-(dicyanomethylidene)indan-1-one derivatives **4a-f** showed in all cases the formation of a single stereoisomer. A X-ray diffraction study on compound **4d** revealed a *Z*-configuration for the carbon-carbon double bond generated during the Knoevenagel condensation process (see Fig. 3). This selectivity is probably associated with steric grounds, since in the *Z*-configuration the steric repulsions between the dicyanomethylidene group (much bulkier than the carbonyl oxygen atom) and the aryl substituents are minimized.[15] In the structure, the butadiene moiety reflects to some extent the π-electron delocalization that exists in the molecule, as indicated by the slightly longer C(1)-C(13) (1.376(2) Å) and C(14)-C(15) (1.373(2) Å), and shorter C(13)-C(14) (1.417(2) Å), bond lengths in comparison to those found for the C=C and C-C bonds in the parent unsubstituted 1,3-butadiene (1.341 and 1.463 Å, respectively).[16]

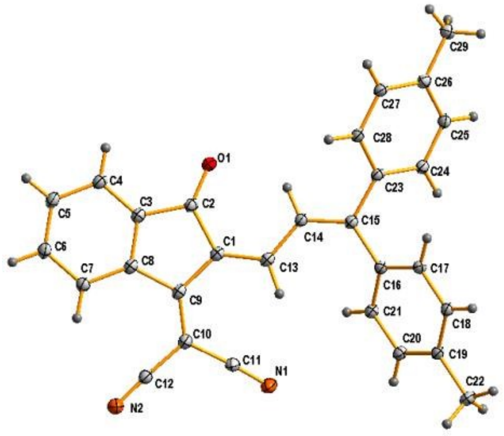

Fig. 3 ORTEP-type view of the structure of **4d** showing the crystallographic labelling scheme. Thermal ellipsoids are drawn at 30% probability level. Selected bond distances (Å): C(2)-O(1) = 1.221(2), C(9)-C(10) = 1.369(2), C(10)-C(11) = 1.444(2), C(10)-C(12) = 1.437(2), C(11)-N(1) = 1.154(2), C(12)-N(2) = 1.417(2), C(1)-C(13) = 1.376(2), C(13)-C(14) = 1.417(2), C(14)-C(15) = 1.373(2). Selected bond angles (°): C(2)-C(1)-C(9) = 106.9(1), C(2)-C(1)-C(13) = 124.6(2), C(9)-C(1)-C(13) = 128.3(2), C(1)-C(13)-C(14) = 123.6(1), C(13)-C(14)-C(15) = 127.4(1), C(14)-C(15)-C(16) = 125.8(1), C(14)-C(15)-C(23) = 116.8(1), C(10)-C(11)-N(1) = 176.2(2), C(10)-C(12)-N(2) = 177.1(2).

The structure of the 1,3-bis(dicyanomethylidene)indane derivative **5b** was also unambiguously confirmed by X-ray diffraction (see Fig. 4), the bond distances within the butadiene chain being in this case 1.359(2) Å (C(1)-C(16)), 1.430(2) Å (C(16)-C(17)) and 1.360(2) Å (C(17)-C(18)).

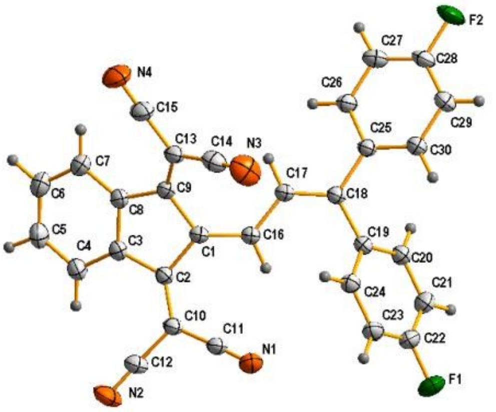

Fig. 4 ORTEP-type view of the structure of **5b** showing the crystallographic labelling scheme. Thermal ellipsoids are drawn at 30% probability level. Selected bond distances (Å): C(2)-C(10) = 1.358(2), C(10)-C(11) = 1.431(2), C(10)-C(12) = 1.428(2), C(11)-N(1) = 1.148(2), C(12)-N(2) = 1.137(2), C(9)-C(13) = 1.360(2), C(13)-C(14) = 1.429(2), C(13)-C(15) = 1.431(2), C(14)-N(3) = 1.143(2), C(15)-N(4) = 1.136(2), C(1)-C(16) = 1.359(2), C(16)-C(17) = 1.430(2), C(17)-C(18) = 1.360(2). Selected bond angles (°): C(2)-C(1)-C(9) = 105.3(1), C(9)-C(1)-C(16) = 128.1(1), C(2)-C(1)-C(16) = 124.5(1), C(1)-C(16)-C(17) = 126.5(1), C(16)-C(17)-C(18) = 124.9(1), C(17)-C(18)-C(19) = 121.4(1), C(17)-C(18)-C(25) = 120.3(1), C(10)-C(11)-N(1) = 176.9(1), C(10)-C(12)-N(2) = 176.8(2), C(13)-C(14)-N(3) = 175.7(2), C(13)-C(15)-N(4) = 178.6(2).

Similarly to other push-pull butadienes,[9,14,17] compounds **4-5a-f** are strongly colored materials in the solid state (from red to blue) that display intense absorption bands in the visible region of their electronic spectra (see Fig. 5). Data of the absorption maxima and molar absorption coefficients measured in dichloromethane solution are collected in Table 1. Compared to the indan-1,3-dione-based butadiene dyes **A** previously reported by us (Scheme 1),[9] the introduction of the dicyanomethylidene groups caused a marked red-shift of the absorption wavelengths. In particular, the replacement of one of the keto units in **A** by the dicyanomethylidene fragment (compounds **4a-f**) results in a bathochromic shift of the maximum absorption band of 59-101 nm, pointing clearly out the strong influence that the acceptor group exerts in the optical properties of these diaryl-substituted butadienes. However, we must note that the effect of replacing the keto group in **4a-f** by an additional dicyanomethylidene moiety, *i.e.* compounds **5a-f**, is not so marked ($\Delta\lambda_{max}$ = 9-31 nm). This fact may be ascribed to the loss of π-conjugation in **5a-f** caused by the intramolecular repulsion between the two electron-withdrawing dicyanomethylidene units.[18]

Table 1 Light absorption properties of the butadiene dyes **4-5a-f**[a]

Compound	λ_{max} (nm)	ε (M^{-1} cm^{-1})
4a	466	34660
4b	465	36380
4c	463	28240
4d	490	38010
4e	523	31770
4f	666	39570
5a	476	25160
5b	474	28760
5c	474	26220
5d	501	20000
5e	544	12680
5f	697	21750

[a] Measured in 6 x 10^{-5} M dichloromethane solution.

With regard to the effect of the *para*-substituents in the phenyl rings, strong bathochromic shifts are observed in both families when the electron-donating groups Me, OMe and NMe_2 are present (compounds **4-5d-f** *vs* **4-5a-c**), existing good linear correlations between Hammett coefficients[19] and λ_{max} values (*r* = 0.9652 for **4a-f** and 0.9643 for **5a-f**; see Fig. 6 and Fig. S2 in the ESI). In this regard, it is worthy of note that compounds **4-5f**, containing the strongest electron-donor dimethylamino group, absorb almost in the near-IR (NIR) region (λ_{max} = 666 and 697 nm, respectively).[20]

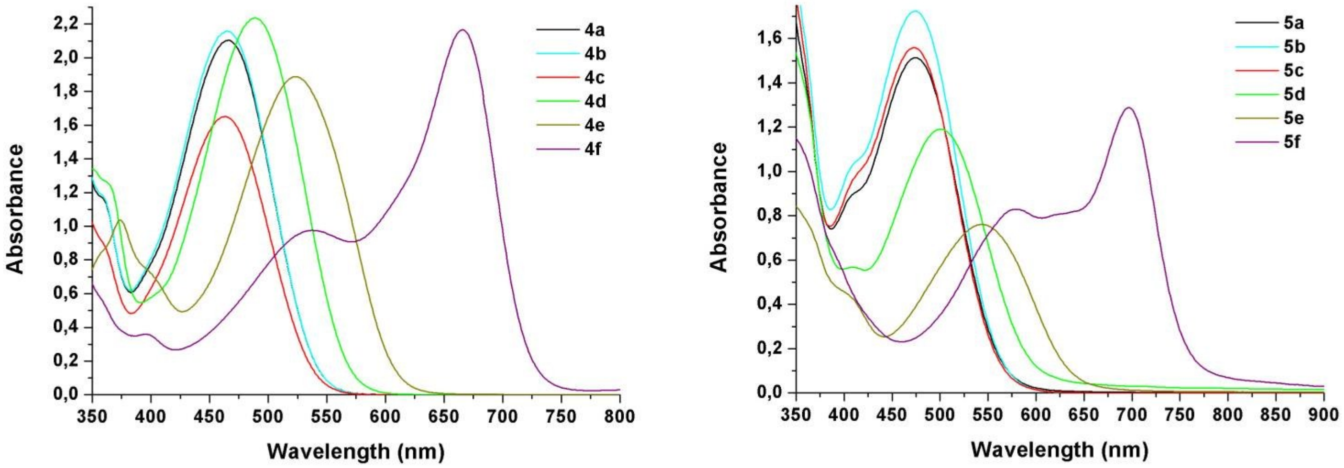

Fig. 5 UV-Vis spectra of the butadiene dyes **4a-f** (left) and **5a-f** (right) recorded in 6 x 10^{-5} M dichloromethane solution.

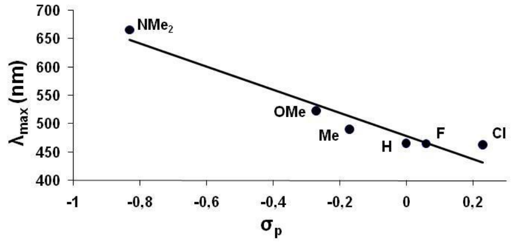

Fig. 6 Plot of λ_{max} *vs* Hammett coefficients for compounds **4a-f**.

The solvatochromic properties of these new push-pull butadiene dyes were evaluated using compounds **4-5f**, absorbing in the longest wavelength region, as models. To this end, UV-Vis spectra were recorded in 23 solvents with different polarities. Although the individual bands in the spectra are overlapped (see the absorption spectra of **4-5f** depicted in Fig. 5), they could be resolved by decomposition of the spectrum in the sum of Gaussian functions, after applying a smoothing spline algorithm to the observed data, followed by a derivative spectroscopy numerical method (only the negative peaks of the second derivatives of the smoothed spectra were used for the estimation of the position of the bands).[21]

Table 2 λ_{max} (nm) values of butadiene dyes **4f** and **5f** in different solvents together with SPP values of the solvents[a]

Entry	Solvent	4f	5f	SPP
1	*n*-Hexane	633	669	0.519
2	Carbon tetrachloride	648	683	0.632
3	Toluene	658	691	0.655
4	Benzene	660	693	0.667
5	Diethyl ether	652	686	0.694
6	1,4-Dioxane	656	690	0.701
7	Chloroform	671	700	0.786
8	Ethyl acetate	664	695	0.795
9	Chlorobenzene	673	702	0.824
10	1-Butanol	673	702	0.837
11	Tetrahydrofuran	671	700	0.838
12	2-Propanol	671	700	0.848
13	Ethanol	672	701	0.853
14	Methanol	671	700	0.857
15	Dichloromethane	673	703	0.876
16	Acetone	674	702	0.881
17	2-Butanone	675	703	0.881
18	Acetonitrile	673	702	0.895
19	Pyridine	679	712	0.922
20	*N,N*-Dimethylformamide	688	713	0.954
21	Benzonitrile	681	712	0.960
22	Nitrobenzene	694	715	0.968
23	Dimethyl sufoxide	693	718	1.00

[a] Spectra recorded using 6 x 10^{-5} M solutions. SPP values were taken from reference 24.

As shown in Table 2, the absorption maxima undergo a large red shift for both compounds with increasing the solvent polarity, *i.e.* $\Delta\lambda_{max}$ = 61 nm for **4f** on going from *n*-hexane to nitrobenzene, and 49 nm for **5f** on going from *n*-hexane to dimethyl sulfoxide. This bathochromic shift of the absorption band, which corresponds with $\pi \rightarrow \pi^*$ electronic spectral transitions (see theoretical calculations below),[22] is related to a greater stabilization of the excited state relative to the ground state with increasing polarity of the solvent. Interestingly, in polar solvents, compound **5f** behaves as a real NIR-absorbing dye with λ_{max} exceeding 700 nm (entries 7 and 9-23).

Different empirical scales (single and multiparametric) of solvent polarity have been established in order to quantify, in a simple way, solvatochromic effects.[23] In this sense, the linear correlation between the solvatochromism of dyes **4-5f** and the most commonly used solvent polarity scales was investigated (hypsochromic scales were excluded in this study). For both compounds the highest linear correlation was obtained with the SPP one, introduced by Catalán and co-workers and based on the positive solvatochromism of 2-(dimethylamino)-7-nitrofluorene and 2-fluoro-7-nitrofluorene.[24] Table 3 and Fig. 7 show the results of the least-squares procedure applied to find the best λ_0 and *s* values, being the adopted mathematical model $\lambda_{max} = \lambda_0 + s\mathrm{SPP}$.[25] The linear correlation coefficient *r* values obtained (0.9616 (**4f**) and 0.9622 (**5f**)) clearly indicate the potential utility of these butadiene dyes as new solvent polarity indicators.[23,26]

Table 3 Fitting results between λ_{max} of dyes **4-5f** in different solvents and SPP values of the solvents[a]

Compound	λ_0	*s*	*r*
4f	579.17 (11.85)	110.50 (14.31)	0.9616
5f	627.91 (9.32)	87.57 (11.25)	0.9622

[a] Values in parentheses represent the 95% confidence limits.

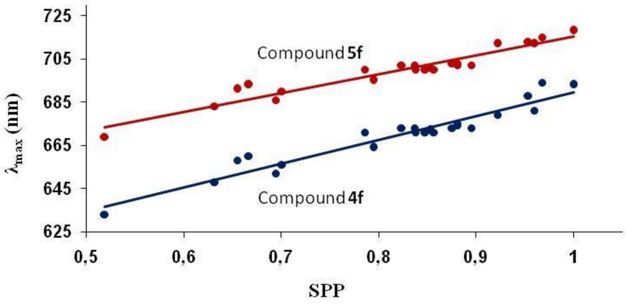

Fig. 7 Plot of λ_{max} *vs* SPP values for compounds **4-5f**.

Finally, we performed DFT calculations on compounds **4-5f** to gain a better understanding of their electronic structures and optical properties. The ground states of these systems were optimized in the gas-phase by using the B3LYP/6-31++G(d) methodology (optimized geometries are included in the ESI file; Fig. S3 and S4). The electronic distributions in the frontier molecular orbitals HOMO-1, HOMO, LUMO and LUMO+1 for **4-5f**, along with their respective energy values, are shown in Fig. 8 and 9, respectively. As expected, the LUMO and LUMO+1 orbitals reside mainly on the 3-(dicyanomethylidene)indan-1-one and 1,3-bis(dicyanomethylidene)indane cores, while the HOMO and HOMO-1 are predominantly located on the dimethylamino-substituted phenyl rings. The gas-phase computed HOMO-

LUMO band gaps of 2.44 (**4f**) and 2.42 eV (**5f**) showed a satisfactory correlation with the UV-Vis data experimentally obtained for these compounds, in which, regardless of the solvent, **5f** absorbed at higher λ_{max}.

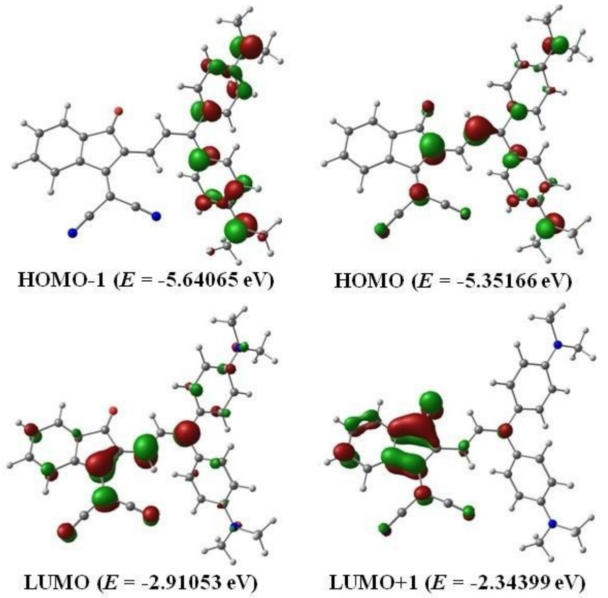

Fig. 8 Frontier orbitals for compound **4f**.

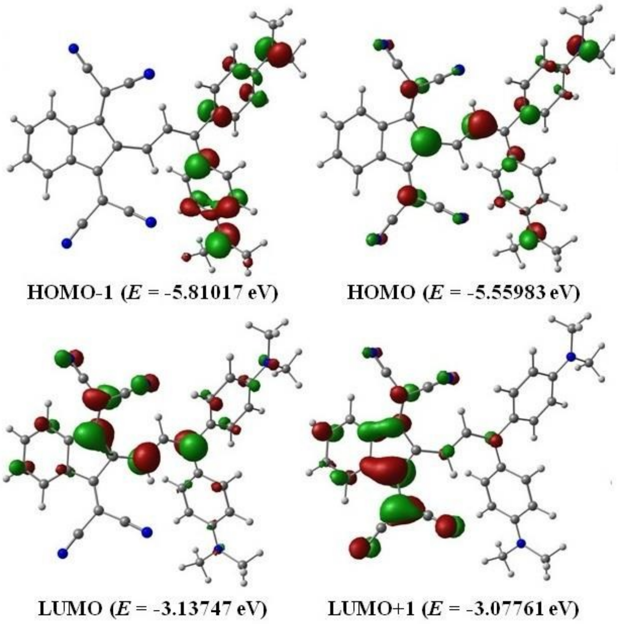

Fig. 9 Frontier orbitals for compound **5f**.

Time-dependent density functional theory (TD-DFT)[27] calculations confirmed that the absorption bands experimentally observed in the UV-Vis spectra of these compounds are mainly related to intramolecular π-electronic transitions between the frontier orbitals depicted in Fig. 8 and 9. The gas-phase computed energies of the vertical excitations, oscillator strengths and orbital contributions are listed in Table 4.

Table 4 Computed excitation energies, oscillator strengths (*f*) and orbital contributions for compounds **4-5f** in the gas phase

Dye	State	eV / nm	*f*	Orbital contributions[a]
4f	1	2.18 / 570	0.463	60% (H→L), 21% (H-1→L), 12% (H→L+1)
	2	2.44 / 509	0.471	63% (H-1→L), 16% (H→L), 11% (H→L+1)
	3	2.58 / 480	0.250	65% (H→L+1), 11% (H→L)
5f	1	2.04 / 608	0.047	56% (H→L+1), 35% (H→L)
	2	2.16 / 574	0.566	51% (H→L), 31% (H→L+1), 19% (H-1→L), 10% (H-1→L+1)
	3	2.34 / 530	0.042	52% (H-1→L+1), 47% (H-1→L)
	4	2.40 / 516	0.445	46% (H-1→L+1), 44% (H-1→L)

[a] H = HOMO, L = LUMO, H-1 = HOMO-1, L+1 = LUMO+1.

Conclusions

In summary, in this paper we have described the preparation of two novel series of push-pull 1,1-diaryl-substituted butadiene dyes containing 3-(dicyanomethylidene)indan-1-one and 1,3-bis(dicyanomethylidene)indane as the acceptor units, and the evaluation of their light absorption properties. The solvatochromic behaviour of two representatives, substituted in the aryl rings by strong electron-donating dimethylamino groups, was studied in detail employing several solvents of different polarity, showing both of them a great sensitivity to this effect and a good linear correlation between their λ_{max} absorptions and the SPP solvent polarity scale. Interestingly, one of them behaved in polar solvents as a NIR-absorbing dye. Due to their easy access and their pronounced and linear solvatochromic properties, these compounds are clear candidates for application as solvent polarity probes.

Experimental

General methods

The manipulations were performed under argon atmosphere using vacuum-line and standard Schlenk techniques. Solvents were dried by standard methods and distilled under nitrogen before use. Enals **1a-f**,[11] 3-(dicyanomethylidene)indan-1-one (**2**)[12b] and 1,3-bis(dicyanomethylidene)indane (**3**)[12b] were prepared following the methods previously reported in the literature. Elemental analyses and HRMS spectra were provided by the Analytical Service of the Instituto de Investigaciones Químicas (IIQ-CSIC) of Seville. Infrared spectra were recorded on a Perkin-Elmer 1720-XFT spectrometer. NMR spectra were recorded on Bruker DPX-300 or AV400 instruments. The chemical shift values (δ) are given in parts per million and are referred to the residual peak of the deuterated solvent employed (^{1}H and ^{13}C) or to the $CFCl_3$ standard (^{19}F). DEPT experiments have been carried out for all the compounds reported. UV-Vis spectra were linearly recorded in wavelength on a Perkin-Elmer Lambda 20 spectrometer at 20 °C using a matched pair of quartz cells with 1 cm in path length. All mathematical analyses (smoothing splines, second derivatives and linear regressions) were performed with MATLAB R2012b.

Synthesis of the 3-(dicyanomethylidene)indan-1-one-based dyes 4a-f

To a solution of the corresponding enal **1a-f** (1 mmol) in ethanol (15 mL), 3-(dicyanomethylidene)indan-1-one (**2**; 0.194 g, 1 mmol) and morpholine (4.4 µL, 0.05 mmol) were added, and the resulting solution stirred at room temperature for 4 h. After evaporation of the solvent, the solid residue was washed with *n*-hexane (2 x 5 mL) and diethyl ether (5 mL), and vacuum-dried. (**4a**): Red solid. Yield: 0.327 g (85%). IR (KBr): v = 1544 (m, C=C), 1589 (m, C=C), 1699 (s, C=O), 2219 (m, C≡N) cm^{-1}. ^1H NMR ($CDCl_3$): δ = 7.31-7.55 (m, 10H, CH_{arom}), 7.79 (m, 2H, CH_{arom}), 7.96 and 8.67 (m, 1H each, CH_{arom}), 8.40 and 8.86 (d, 1H each, $^3J_{HH}$ = 11.9 Hz, =CH) ppm. $^{13}C\{^1H\}$ NMR ($CDCl_3$): δ = 71.1 (C), 113.4 (CN), 114.3 (CN), 123.1 (CH), 123.9 (CH), 125.2 (CH), 127.0 (C), 128.6 (CH), 128.7 (CH), 129.6 (CH), 129.7 (CH), 130.7 (CH), 134.5 (CH), 135.2 (CH), 137.0 (C), 137.4 (C), 139.8 (C), 140.5 (C), 144.6 (CH), 159.8 (C), 163.6 (C), 189.1 (CO) ppm. Elemental analysis calcd (%) for $C_{27}H_{16}N_2O$: C 84.36, H 4.20, N 7.29; found: C 84.25, H 4.25, N 7.40. HRMS (Electrospray): *m/z* 385.1345 [M^+ + H], $C_{27}H_{17}N_2O$ requires 385.1341. (**4b**): Red solid. Yield: 0.366 g (87%). IR (KBr): v = 1563 (m, C=C), 1589 (m, C=C), 1694 (s, C=O), 2220 (m, C≡N) cm^{-1}. ^1H NMR ($CDCl_3$): δ = 7.09-7.31 (m, 6H, CH_{arom}), 7.49 and 7.78 (m, 2H each, CH_{arom}), 7.95 and 8.68 (m, 1H, CH_{arom}), 8.33 and 8.76 (d, 1H each, $^3J_{HH}$ = 11.8 Hz, =CH) ppm. $^{13}C\{^1H\}$ NMR ($CDCl_3$): δ = 73.4 (C), 115.5 (CN), 116.2 (CN), 117.9 (d, $^2J_{CF}$ = 21.2 Hz, CH), 118.2 (d, $^2J_{CF}$ = 21.2 Hz, CH), 125.0 (CH), 126.0 (CH), 127.4 (CH), 129.4 (C), 133.6 (d, $^3J_{CF}$ = 8.5 Hz, CH), 134.7 (d, $^3J_{CF}$ = 8.5 Hz, CH), 136.7 (CH), 137.4 (CH), 138.7 (C), 139.4 (C), 141.9 (C), 145.9 (CH), 161.8 (C), 162.7 (C), 168.5 (d, $^1J_{CF}$ = 251.1 Hz, C), 166.4 (d, $^1J_{CF}$ = 253.2 Hz, C), 191.2 (CO) ppm. $^{19}F\{^1H\}$ NMR ($CDCl_3$): δ = -110.0 (s), -108.4 (s) ppm. Elemental analysis calcd (%) for $C_{27}H_{14}F_2N_2O$: C 77.14, H 3.36, N 6.66; found: C 77.25, H 3.29, N 6.80. HRMS (Electrospray): *m/z* 421.1147 [M^+ + H], $C_{27}H_{15}F_2N_2O$ requires 421.1152. (**4c**): Red solid. Yield: 0.376 g (83%). IR (KBr): v = 1559 (m, C=C), 1583 (m, C=C), 1698 (s, C=O), 2223 (m, C≡N) cm^{-1}. ^1H NMR ($CDCl_3$): δ = 7.24-7.54 (m, 8H, CH_{arom}), 7.81 (m, 2H, CH_{arom}), 7.96 and 8.70 (m, 1H each, CH_{arom}), 8.33 and 8.82 (d, 1H each, $^3J_{HH}$ = 11.8 Hz, =CH) ppm. $^{13}C\{^1H\}$ NMR ($CDCl_3$): δ = 73.8 (C), 115.5 (CN), 116.1 (CN), 125.4 (CH), 126.1 (CH), 127.4 (CH), 129.5 (C), 129.8 (CH), 130.0 (CH), 130.1 (CH), 131.1 (CH), 131.4 (CH), 132.7 (C), 134.0 (CH), 136.7 (C), 137.1 (C), 137.5 (C), 139.2 (C), 140.7 (C), 141.9 (C), 145.3 (CH), 162.0 (C), 191.1 (CO) ppm. Elemental analysis calcd (%) for $C_{27}H_{14}Cl_2N_2O$: C 71.54, H 3.11, N 6.18; found: C 71.66, H 3.06, N 6.30. HRMS (Electrospray): *m/z* 453.0556 [M^+ + H], $C_{27}H_{15}Cl_2N_2O$ requires 453.0561. (**4d**): Red solid. Yield: 0.363 g (88%). IR (KBr): v = 1558 (m, C=C), 1588 (m, C=C), 1699 (s, C=O), 2215 (m, C≡N) cm^{-1}. ^1H NMR ($CDCl_3$): δ = 2.44 and 2.48 (s, 3H each, CH_3), 7.19-7.44 (m, 8H, CH_{arom}), 7.77 (m, 2H, CH_{arom}), 7.93 and 8.65 (m, 1H each, CH_{arom}), 8.40 and 8.79 (d, 1H each, $^3J_{HH}$ = 12.1 Hz, =CH) ppm. $^{13}C\{^1H\}$ NMR ($CDCl_3$): δ = 21.5 (s, CH_3), 70.5 (C), 113.7 (CN), 114.6 (CN), 122.4 (CH), 123.8 (CH), 125.2 (CH), 126.4 (C), 129.5 (CH), 129.9 (CH), 131.0 (CH), 134.4 (CH), 135.1 (CH), 137.5 (C), 138.1 (C), 139.9 (C), 140.2 (C), 141.6 (C), 145.4 (CH), 160.2 (C), 164.5 (C), 189.3 (CO) ppm. Elemental analysis calcd (%) for $C_{29}H_{20}N_2O$: C 84.44, H 4.89, N 6.79; found: C 84.59, H 4.91, N 7.85. HRMS (Electrospray): *m/z* 413.1659 [M^+ + H], $C_{29}H_{21}N_2O$ requires 413.1654. (**4e**): Purple solid. Yield: 0.355 g (80%). IR (KBr): v = 1542 (m, C=C), 1584 (m, C=C), 1695 (s, C=O), 2213 (m, C≡N) cm^{-1}. ^1H NMR ($CDCl_3$): δ = 3.88 and 3.91 (s, 3H each, OCH_3), 6.93, 7.03, 7.26 and 7.49 (d, 2H each, $^3J_{HH}$ = 8.5 Hz, CH_{arom}), 7.73 (m, 2H, CH_{arom}), 7.90 and 8.63 (m, 1H each, CH_{arom}), 8.38 and 8.71 (d, 1H each, $^3J_{HH}$ = 12.0 Hz, =CH) ppm. $^{13}C\{^1H\}$ NMR ($CDCl_3$): δ = 55.5 (s, OCH_3), 69.6 (C), 114.0 (CH), 114.2 (CH), 114.3 (CN), 114.8 (CN), 121.6 (CH), 123.7 (CH), 125.1 (CH), 125.4 (C), 129.6 (C), 132.0 (CH), 132.8 (CH), 133.5 (C), 134.2 (CH), 134.9 (CH), 137.4 (C), 138.9 (C), 145.0 (CH), 160.3 (C), 161.4 (C), 162.3 (C), 164.5 (C), 189.4 (CO) ppm. Elemental analysis calcd (%) for $C_{29}H_{20}O_3N_2$: C 78.36, H 4.54, N 6.30; found: C 78.29, H 4.66, N 6.42. HRMS (Electrospray): *m/z* 445.1563 [M^+ + H], $C_{29}H_{21}O_3N_2$ requires 445.1552. (**4f**): Blue solid. Yield: 0.367 g (78%). IR (KBr): v = 1595 (s, C=C), 1686 (s, C=O), 2211 (m, C≡N) cm^{-1}. ^1H NMR ($CDCl_3$): δ = 3.11 (s, 12H, $N(CH_3)_2$), 6.70 and 7.26 (d, 2H each, $^3J_{HH}$ = 7.4 Hz, CH_{arom}), 6.79 and 7.52 (d, 2H each, $^3J_{HH}$ = 7.7 Hz, CH_{arom}), 7.66 (m, 2H, CH_{arom}), 7.83 and 8.60 (m, 1H each, CH_{arom}), 8.40 and 8.66 (d, 1H each, $^3J_{HH}$ = 12.5 Hz, =CH) ppm. $^{13}C\{^1H\}$ NMR ($CDCl_3$): δ = 42.1 (s, $N(CH_3)_2$), 79.2 (C), 113.5 (CH), 113.7 (CH), 117.1 (CN), 118.0 (CN), 122.1 (CH), 123.7 (CH), 124.9 (CH), 126.6 (CH), 127.2 (CH), 130.5 (C), 130.8 (C), 132.9 (C), 135.3 (CH), 136.0 (CH), 139.3 (C), 141.9 (C), 149.4 (CH), 154.4 (C), 154.7 (C), 163.0 (C), 170.6 (C), 191.8 (CO) ppm. Elemental analysis calcd (%) for $C_{31}H_{26}N_4O$: C 79.12, H 5.57, N 11.91; found: C 79.23, H 5.64, N 12.02. HRMS (Electrospray): *m/z* 471.2185 [M^+ + H], $C_{31}H_{27}N_4O$ requires 471.2185.

Synthesis of the 1,3-bis(dicyanomethylidene)indane-based dyes 5a-f

To a solution of the corresponding enal **1a-f** (1 mmol) in acetic anhydride (12 mL), 1,3-bis(dicyanomethylidene)indane (**3**; 0.242 g, 1 mmol) was added, and the resulting solution stirred at 60 °C for 6 h. After evaporation of the solvent, the solid residue was washed with *n*-hexane (2 x 5 mL) and diethyl ether (5 mL), and vacuum-dried. (**5a**): Red solid. Yield: 0.398 g (92%). IR (KBr): v = 1590 (s, C=C), 2213 (m, C≡N), 2215 (m, C≡N) cm^{-1}. ^1H NMR ($CDCl_3$): δ = 7.01 and 8.04 (d, 1H each, $^3J_{HH}$ = 11.4 Hz, =CH), 7.28-7.56 (m, 10H, CH_{arom}), 7.79 and 8.58 (m, 2H each, CH_{arom}) ppm. $^{13}C\{^1H\}$ NMR ($CDCl_3$): δ = 74.1 (C), 78.8 (C), 114.6 (CN), 114.9 (CN), 115.2 (CN), 115.3 (CN), 127.2 (CH), 127.4 (CH), 127.9 (CH), 130.8 (CH), 130.9 (CH), 131.8 (CH), 132.6 (CH), 133.1 (CH), 133.3 (C), 133.5 (CH), 136.5 (CH), 136.8 (CH), 138.5 (C), 139.3 (C), 139.9 (C), 142.3 (C), 144.2 (CH), 162.8 (C), 163.0 (C), 164.9 (C) ppm. Elemental analysis calcd (%) for $C_{30}H_{16}N_4$: C 83.32, H 3.73, N 12.95; found: C 83.44, H 3.80, N 13.13. HRMS (Electrospray): *m/z* 433.1453 [M^+ + H], $C_{30}H_{17}N_4$ requires 433.1453. (**5b**): Red solid. Yield: 0.403 g (86%). IR (KBr): v = 1567 (m, C=C), 1597 (m, C=C), 2230 (m, C≡N), 2234 (m, C≡N) cm^{-1}. ^1H NMR ($CDCl_3$): δ = 6.91 and 8.00 (d, 1H each,

$^{3}J_{HH}$ = 11.6 Hz, =CH), 7.11-7.46 (m, 8H, CH$_{arom}$), 7.78 and 8.59 (m, 2H each, CH$_{arom}$) ppm. ^{13}C{^{1}H} NMR (CDCl$_3$): δ = 72.3 (C), 77.2 (C), 112.7 (CN), 112.9 (CN), 113.1 (CN), 113.2 (CN), 116.1 (d, $^{2}J_{CF}$ = 21.8 Hz, CH), 116.3 (d, $^{2}J_{CF}$ = 21.8 Hz, CH), 125.1 (CH), 125.4 (CH), 125.9 (CH), 131.7 (s, C), 131.8 (d, $^{3}J_{CF}$ = 8.9 Hz, CH), 131.1 (d, $^{4}J_{CF}$ = 3.4 Hz, C), 133.5 (d, $^{3}J_{CF}$ = 8.9 Hz, CH), 134.7 (CH), 134.9 (CH), 136.4 (d, $^{4}J_{CF}$ = 3.6 Hz, C), 136.5 (C), 137.8 (C), 141.4 (CH), 159.8 (C), 160.7 (C), 161.0 (C), 164.2 (d, $^{1}J_{CF}$ = 252.7 Hz, C), 164.6 (d, $^{1}J_{CF}$ = 253.8 Hz, C) ppm. ^{19}F{^{1}H} NMR (CDCl$_3$): δ = -108.4 (s), -107.9 (s) ppm. Elemental analysis calcd (%) for $C_{30}H_{14}N_4F_2$: C 76.92, H 3.01, N 11.96; found: C 77.09, H 3.15, N 12.10. HRMS (Electrospray): *m/z* 469.1260 [M$^+$ + H], $C_{30}H_{15}N_4F_2$ requires 469.1265. (**5c**):[13] Red solid. Yield: 0.406 g (81%). IR (KBr): *v* = 1557 (m, C=C), 1599 (m, C=C), 2222 (m, C≡N) cm^{-1}. ^{1}H NMR (CDCl$_3$): δ = 6.94 and 7.95 (d, 1H each, $^{3}J_{HH}$ = 11.6 Hz, =CH), 7.25-7.52 (m, 8H, CH$_{arom}$), 7.80 and 8.57 (m, 2H each, CH$_{arom}$) ppm. ^{13}C{^{1}H} NMR (CDCl$_3$): δ = 72.7 (C), 77.2 (C), 112.6 (CN), 112.8 (CN), 112.9 (CN), 113.1 (CN), 125.4 (CH), 125.5 (CH), 126.0 (CH), 129.3 (CH), 129.5 (CH), 130.8 (CH), 132.3 (C), 132.6 (CH), 134.8 (CH), 135.0 (CH), 135.2 (C), 136.5 (C), 137.1 (C), 137.6 (C), 137.8 (C), 138.4 (C), 140.7 (CH), 159.1 (C), 160.7 (C), 161.0 (C) ppm. Elemental analysis calcd (%) for $C_{30}H_{14}Cl_2N_4$: C 71.87, H 2.81, N 11.17; found: C 71.94, H 2.77, N 11.32. HRMS (Electrospray): *m/z* 501.0675 [M$^+$ + H], $C_{30}H_{15}Cl_2N_4$ requires 501.0674. (**5d**): Red solid. Yield: 0.391 g (85%). IR (KBr): *v* = 1567 (m, C=C), 1594 (m, C=C), 2195 (m, C≡N), 2225 (m, C≡N) cm^{-1}. ^{1}H NMR (CDCl$_3$): δ = 2.44 and 2.48 (s, 3H each, CH$_3$), 6.94 and 8.05 (d, 1H each, $^{3}J_{HH}$ = 11.6 Hz, =CH), 7.23-7.38 (m, 8H, CH$_{arom}$), 7.79 and 8.57 (m, 2H each, CH$_{arom}$) ppm. ^{13}C{^{1}H} NMR (CDCl$_3$): δ = 21.5 (s, CH$_3$), 21.6 (s, CH$_3$), 71.4 (C), 76.1 (C), 112.9 (CN), 113.0 (CN), 113.5 (CN), 113.6 (CN), 124.6 (CH), 125.3 (CH), 125.8 (CH), 129.5 (CH), 129.6 (CH), 130.0 (CH), 130.4 (C), 131.8 (CH), 134.4 (CH), 134.5 (C), 134.6 (CH), 136.6 (C), 137.8 (C), 137.9 (C), 141.3 (C), 142.0 (C), 142.9 (CH), 161.0 (C), 163.8 (C) ppm. Elemental analysis calcd (%) for $C_{32}H_{20}N_4$: C 83.46, H 4.38, N 12.17; found: C 83.58, H 4.27, N 12.31. HRMS (Electrospray): *m/z* 461.1765 [M$^+$ + H], $C_{32}H_{21}N_4$ requires 461.1766. (**5e**): Purple solid. Yield: 0.453 g (92%). IR (KBr): *v* = 1557 (m, C=C), 1589 (m, C=C), 2194 (m, C≡N), 2202 (m, C≡N) cm^{-1}. ^{1}H NMR (CDCl$_3$): δ = 3.91 (br s, 6H, OCH$_3$), 6.88 and 8.09 (d, 1H each, $^{3}J_{HH}$ = 11.4 Hz, =CH), 6.97-7.44 (m, 8H, CH$_{arom}$), 7.75 and 8.57 (m, 2H each, CH$_{arom}$) ppm. ^{13}C{^{1}H} NMR (CDCl$_3$): δ = 55.6 (s, OCH$_3$), 70.5 (C), 75.1 (C), 113.2 (CN), 113.3 (CN), 113.7 (CN), 113.8 (CN), 114.4 (CH), 114.5 (CH), 124.1 (CH), 125.2 (CH), 125.7 (CH), 129.2 (C), 130.0 (C), 132.2 (CH), 132.9 (C), 133.8 (CH), 134.2 (CH), 134.4 (CH), 136.6 (C), 138.0 (C), 143.6 (CH), 161.0 (C), 162.3 (C), 162.6 (C), 163.9 (C), 166.4 (C) ppm. Elemental analysis calcd (%) for $C_{32}H_{20}N_4O_2$: C 78.03, H 4.09, N 11.38; found: C 77.91, H 4.16, N 11.49. HRMS (Electrospray): *m/z* 493.1666 [M$^+$ + H], $C_{32}H_{21}N_4O_2$ requires 493.1665. (**5f**): Blue solid. Yield: 0.487 g (94%). IR (KBr): *v* = 1591 (s, C=C), 2191 (m, C≡N), 2210 (m, C≡N) cm^{-1}. ^{1}H NMR (CDCl$_3$): δ = 3.15 (s, 12H, N(CH$_3$)$_2$), 6.72 (m, 4H, CH$_{arom}$), 6.78 and 8.18 (d, 1H each, $^{3}J_{HH}$ = 12.6 Hz, =CH), 7.36-7.45 (m, 4H, CH$_{arom}$), 7.63 and 8.53 (m, 2H each, CH$_{arom}$) ppm. ^{13}C{^{1}H} NMR (CDCl$_3$): δ = 40.4 (s, N(CH$_3$)$_2$), 67.9 (C), 77.0 (C), 111.6 (CH), 111.8 (CH), 114.6 (CN), 115.3 (CN), 123.7 (C), 114.5 (CH), 124.5 (CH), 124.9 (CH), 133.0 (CH), 134.2 (C), 135.9 (C), 137.8 (C), 145.7 (CH), 153.3 (C), 160.5 (C), 169.2 (C) ppm. Elemental analysis calcd (%) for $C_{34}H_{26}N_6$: C 78.74, H 5.05, N 16.20; found: C 78.87, H 5.12, N 16.31. HRMS (Electrospray): *m/z* 519.2283 [M$^+$ + H], $C_{34}H_{27}N_6$ requires 519.2297.

Computational details

All the theoretical calculations have been performed using the density functional theory (DFT). Becke´s three-parameter exchange functional (B3)[28] in conjunction with the Lee-Yang-Parr correlation functional (LYP)[29] was employed as implemented in Gaussian 03.[30] All structures were optimized in the gas-phase by using bond lengths and angles from the X-ray data of analogous compounds herein described (see below). In all geometry optimizations 6-31++G(d) basis set was used for all the atoms.[31] Frequency calculations were performed to determine whether the optimized geometries were minima on the potential energy surface.

Time dependent density functional theory (TD-DFT)[27] single points calculations were performed using the B3LYP functional and the 6-31++G(d) basis set on the optimized structures at the same level to obtain the calculated λ_{max} values. The 40 lowest-energy excited states were computed for all the molecules. Molecular orbital contours were plotted using Chemcraft 1.7.[32]

X-Ray crystal structure determination of compounds 4d and 5b

Crystals of **4d** and **5b** suitable for X-ray diffraction analysis were obtained by slow diffusion of *n*-hexane into saturated solutions of the compounds in ethyl acetate and in dichloromethane, respectively. The most relevant crystal and refinement data are collected in Table 5. In both cases, data collection was performed with an Oxford Diffraction Xcalibur Nova single crystal diffractometer using Cu-Kα radiation (λ = 1.5418 Å). Images were collected at a fixed crystal-to-detector distance of 65 mm, using the oscillation method with 1° oscillation and 1.5-45 s variable exposure time per image for **4d**, and 8.6-60 s for **5b**. Data collection strategy was calculated with the program CrysAlis Pro CCD.[33] Data reduction and cell refinement was performed with the program CrysAlis Pro RED.[33] An empirical absorption correction was applied using the SCALE3 ABSPACK algorithm as implemented in the program CrysAlis Pro RED.[33]

In both cases, the software package WINGX was used for space group determination, structure solution, and refinement.[34] The structures were solved by direct methods and conventional Fourier techniques, and refined by full-matrix least-squares on F^2 using SHELXL97.[35] During the final stages of the refinements, all the positional parameters and the anisotropic temperature factors of all non-H atoms were refined. The coordinates of the H atoms were found from difference Fourier maps and included in the refinements with isotropic temperature parameters. The function minimized was $\{\Sigma[\omega(F_o^2 - F_c^2)^2]/\Sigma[\omega(F_o^2)^2]\}^{1/2}$ where $\omega = 1/[\sigma^2(F_o^2) + (aP)^2$

+ bP] (a and b values are collected in Table 5) with $\sigma(F_o^2)$ from counting statistics and P = [Max $(F_o^2,0)$ + $2F_c^2$]/3. Atomic scattering factors were taken from International Tables for X-ray Crystallography.[36] Geometrical calculations were made with PARST.[37] The crystallographic plots were made with DIAMOND.[38]

Table 5 Crystal data and structure refinement for compounds **4d** and **5b**

	4d	**5b**
Empirical formula	$C_{29}H_{20}N_2O$	$C_{30}H_{14}N_4F_2$
Formula weight	412.47	468.45
Temperature/K	293(2)	297(2)
Wavelength/Å	1.54184	1.54184
Crystal system	Triclinic	Triclinic
Space group	P-1	P-1
Crystal size/mm	0.39 x 0.04 x 0.03	0.31 x 0.11 x 0.05
a/Å	9.0687(6)	5.4077(2)
b/Å	10.7492(7)	9.7318(3)
c/Å	12.4386(13)	22.3871(6)
α (°)	114.884(8)	89.248(2)
β(°)	102.785(7)	89.554(3)
γ(°)	95.489(5)	80.152(3)
Z	2	2
Volume/Å^3	1047.90(16)	1160.68(6)
Calculated density/g cm^{-3}	1.307	1.340
μ/mm^{-1}	0.624	0.757
F(000)	432	480
ϑ range/°	4.094-73.683	3.950-74.375
Index ranges	$-7 \le h \le 10$	$-6 \le h \le 6$
	$-12 \le k \le 13$	$-12 \le k \le 11$
	$-14 \le l \le 15$	$-26 \le l \le 27$
Completeness to ϑ_{max}	93.2%	96.9%
No. of reflns. collected	7818	13086
No. of unique reflns.	3953 (R_{int} = 0.046)	4584 (R_{int} = 0.023)
No. of parameters/restraints	299/0	381/0
Refinement method	Full-matrix least-squares on F^2	
Goodness-of-fit on F^2	1.014	1.040
Weight function (a, b)	0.1096, 0.0000	0.0744, 0.1323
R_1 [I> 2σ(I)]^a	0.0512	0.0446
wR_2 [I> 2σ(I)]^a	0.1398	0.1175
R_1 (all data)	0.0635	0.0487
wR_2 (all data)	0.1468	0.1248
Largest diff. peak and hole/e Å^{-3}	0.275, -0.260	0.139, -0.218

$^a R_1 = \sum(|F_o|-|F_c|)/\sum|F_o|$; $wR_2 = \{\sum[w(F_o^2-F_c^2)^2]/\sum[w(F_o^2)^2]\}^{1/2}$

Acknowledgements

This work was supported by the Spanish MINECO (projects CTQ2013-40591-P and CTQ2014-51912-REDC) and the Gobierno del Principado de Asturias (project GRUPIN14-006). J.F. thanks MINECO and ESF for the award of a Juan de la Cierva contract.

Notes and references

1 See, for example: (*a*) *Functional Organic and Polymeric Materials: Molecular Functionality - Macroscopic Reality*, ed. T. H. Richardson, John Wiley & Sons, London, 2000; (*b*) *Organic Electronics: Materials, Manufacturing and Applications*, ed. H. Klauk, Wiley-VCH, Weinheim, 2006; (*c*) *Organic Light Emitting Devices: Synthesis, Properties and Applications*, ed. K. Müllen and U. Scherf, Wiley-VCH, Weinheim, 2006; (*d*) *Functional Organic Materials: Synthesis, Strategies and Applications*, ed. T. J. J. Müller and U. H. F. Bunz, Wiley-VCH, Weinheim, 2007; (*e*) *Handbook of Organic Materials for Optical and (Opto)electronic Devices*, ed. O. Ostroverkhova, Woodhead Publishing Limited, Cambridge, 2013.

2 See, for example: F. Bureš, *RSC Adv.*, 2014, **4**, 58826 and references cited therein.

3 For recent examples, see: (*a*) K. Traskovskis, I. Mihailovs, A. Tomakovs, A. Jurgis, V. Kokars and M. Rutkis, *J. Mater. Chem.*, 2012, **22**, 1268; (*b*) R. M. El-Shishtawy, F. Borbone, Z. M. Al-Amshany, A. Tuzi, A. Barsella, A. M. Asiri and A. Roviello, *Dyes Pigm.*, 2013, **96**, 45; (*c*) V. Zilinskaite, D. Gudeika, J. V. Grazulevicius, D. Volyniuk, G. Buika, V. Jankauskas, G. Juska, M. Rutkis and A. Tokmakov, *Dyes Pigm.*, 2015, **113**, 38; (*d*) K. Traskovskis, E. Zarins, L. Laipniece, A. Tokmakovs, V. Kokars and M. Rutkis, *Mat. Chem. Phys.*, 2015, **155**, 232.

4 For recent examples, see: (*a*) A. Vembris, M. Porozovs, I. Muzikante, V. Kokars and E. Zarins, *J. Photon. Energy*, 2011, 1, 011001/1; (*b*) K. H. Lee, Y. K. Kim and S. S. Yoon, *Bull. Korean Chem. Soc.*, 2011, **32**, 4419; (*c*) E. Zarins, J. Jubels and V. Kokars, *Adv. Mater. Res.*, 2011, **222**, 271; (*d*) H. S. Jang, K. H. Lee, E. J. Na, Y. K. Kim and S. S. Yoon, *Mol. Cryst. Liq. Cryst.*, 2012, **568**, 1.

5 (*a*) I. Paci, J. C. Johnson, X. Chen, G. Rana, D. Popović, D. E. David, A. J. Nozik, M. A. Ratner and J. Michl, *J. Am. Chem. Soc.*, 2006, **128**, 16546; (*b*) S. Matsumoto, T. Aoki, T. Suzuki, M. Akazome, A. Betto and Y. Suda, *Bull. Chem. Soc. Jpn.*, 2012, **85**, 1329; (*c*) N. Shibayama, Y. Inoue, M. Abe, S. Kajiyama, H. Ozawa, H. Miura and H. Arakawa, *Chem. Commun.*, 2015, **51**, 12795.

6 For recent examples, see: (*a*) M. Hirade, T. Yasuda and C. Adachi, *J. Phys. Chem. C*, 2013, **117**, 4986; (*b*) J. Latvels, R. Grzibovskis, A. Vembris and D. Blumberga, *Environ. Climate Technol.*, 2013, **12**, 28; (*c*) A. Arjona-Esteban, J. Krumrain, A. Liess, M. Stolte, L. Huang, D. Schmidt, V. Stepanenko, M. Gsänger, D. Hertel, K. Meerholz and F. Würthner, *J. Am. Chem. Soc.*, 2015, **137**, 13524; (*d*) Y. Kim, C. E. Son, S.-J. Moon and E. Lim, *RSC Adv.*, 2015, **5**, 62739.

7 For recent examples, see: (*a*) A. S. F. Farinha, A. C. Tomé and J. A. S. Cavaleiro, *Tetrahedron Lett.*, 2010, **51**, 2184; (*b*) Y. Lv, Y. Guo, J. Xu and S. Shao, *J. Fluorine Chem.*, 2011, **132**, 973; (*c*) X. Zhou, H. Yang, J. Hao, C. Yin, D. Liu and W. Guo, *Chem. Lett.*, 2012, **41**, 518; (*d*) A. S. F. Farinha, M. R. C. Fernandes and A. C. Tomé, *Sensor Actuat. B-Chem.*, 2014, **200**, 332.

8 (*a*) M.-A. Tehfe, F. Dumur, B. Graff, D. Gigmes, J.-P. Fouassier and J. Lalevée, *Macromolecules*, 2013, **46**, 3332; (*b*) M.-A. Tehfe, F. Dumur, B. Graff, F. Morlet-Savary, J.-P. Fouassier, D. Gigmes and J. Lalevée, *Macromolecules*, 2013, **46**, 3761; (*c*) P. Xiao, F. Dumur, B. Graff, F. Morlet-Savary, L. Vidal, D. Gigmes, J. P. Fouassier and J. Lalevée, *Macromolecules*, 2014, **47**, 26.

9 J. Francos, J. Borge, J. Díez, S. E. García-Garrido and V. Cadierno, *Catal. Commun.*, 2015, **63**, 10.

10 For reviews covering the Meyer-Schuster rearrangement of alkynols, see: (*a*) S. Swaminathan and K. V. Narayanan, *Chem. Rev.*, 1971, **71**, 429; (*b*) D. A. Engel and G. B. Dudley, *Org. Biomol. Chem.*, 2009, **7**, 4149; (*c*) V. Cadierno, P. Crochet, S. E. García-Garrido and J. Gimeno, *Dalton Trans.*, 2010, **39**, 4015; (*d*) E. B. Bauer, *Synthesis*, 2012, **44**, 1131.

11 The ability of $InCl_3$ to promote the catalytic rearrangement of propargylic alcohols in water under microwave (MW) irradiation was discovered by our group some years ago: V. Cadierno, J. Francos and J. Gimeno, *Tetrahedron Lett.*, 2009, **50**, 4773.

12 See, for example: (*a*) G. Irick, *J. Chem. Eng. Data*, 1971, **16**, 118; (*b*) K. A. Bello, L. Cheng and J. Griffiths, *J. Chem. Soc., Perkin Trans. 2*, 1987, 815; (*c*) P. Solanke, F. Bureš, O. Pytela,

M. Klikar, T. Mikysek, L. Mager, A. Barsella and Z. Růžičková, *Eur. J. Org. Chem.*, 2015, 5339 and references cited therein.

13 Only the preparation of compound **5c** (see below), and its behaviour as electrophotographic photoreceptor, has been mentioned in a patent: M. Kuroda, N. Sekine, N. Kotani, K. Okura and Y. Ueno, *Jpn. Pat.*, JP2005035901, 2005.

14 Although limited in number, related monoaryl-substituted butadienic compounds are known: (*a*) T. Suzuki, H. Ono, S. Aramaki, M. Yokoyama and M. Sudo, *Jpn. Pat.*, JP61063846, 1986; (*b*) S. Maeda, Y. Kurose, Y. Kimura and J. Nakakuki, *Jpn. Pat.*, JP63075065, 1988; (*c*) T. Hioki and A. Tomioka, *Jpn. Pat.*, JP01031868, 1989; (*d*) A. Senoo, K. Inai, H. Miyazaki and S. Go, *Jpn. Pat.*, JP02259653, 1990; (*e*) H. Szymusiak, R. Zielinski, B. W. Domagalska and K. A. Wilk, *Comput. Chem.*, 2000, **24**, 369; (*f*) G. Meshulam, G. Berkovic, Z. Kotler, A. Ben-Asuly, R. Mazor, L. Shapiro and V. Khodordovsky, *Synthetic Met.*, 2000, **115**, 219.

15 DFT calculations (B3LYP/6-31++G(d)) on compound **4a** showed that, in gas-phase, the *Z* isomer is *ca.* 3.6 kcal mol^{-1} more stable than the *E* one. Details are given in the ESI file.

16 K. Kuchitsu, T. Fukuyama and Y. Morino, *J. Mol. Struct.*, 1968, **1**, 463.

17 See, for example: (*a*) S. Nakatsuji, K. Nakashima, M. Iyoda and S. Akiyama, *Bull. Chem. Soc. Jpn.*, 1988, **61**, 2253; (*b*) S. Nakatsuji, T. Yahiro, K. Nakashima, S. Akiyama and H. Nakazumi, *Chem. Express*, 1989, **4**, 601; (*c*) S. Nakatsuji, T. Yahiro, K. Nakashima, S. Akiyama and H. Nakazumi, *Bull. Chem. Soc. Jpn.*, 1991, **64**, 1641; (*d*) J. Borge, V. Cadierno, J. Díez, S. E. García-Garrido and J. Gimeno, *Dyes Pigm.*, 2010, **87**, 209.

18 This loss of π-conjugation is in accord with the bond distances found for the butadiene chain in the crystal structure of **5b**, and was also confirmed by measuring the dihedral angle between the planes C(8)-C(9)-C(13) and C(7)-C(8)-C(9) (24.42°), and the planes C(3)-C(2)-C(10) and C(4)-C(3)-C(2) (18.92°) (see Fig. 4). As the deviation of these dihedral angles from 0° increases, the efficiency of the π-orbital overlapping within the acceptor indane unit decreases, causing the loss of π-conjugation in these compounds. To compare, the dihedral angle between the planes C(8)-C(9)-C(10) and C(7)-C(8)-C(9) in the crystal structure of compound **4d** (see Fig. 3) is only 5.43°.

19 C. Hansch, A. Leo and R. W. Taft, *Chem. Rev.*, 1991, **91**, 165.

20 Dyes active in the NIR region (700-1200 nm) are finding important applications, particularly in the biomedical field as imaging systems. See, for example: (*a*) J. Fabian, H. Nakazumi and M. Matsuoka, *Chem. Rev.*, 1992, **92**, 1197; (*b*) J. O. Escobedo, O. Rusin, S. Lim and R. M. Strongin, *Curr. Opin. Chem. Biol.*, 2010, **14**, 64; (*c*) S. Luo, E. Zhang, Y. Su, T. Cheng and C. Shi, *Biomaterials*, 2011, **32**, 7127; (*d*) Z. Guo, S. Park, J. Yoon and I. Shin, *Chem. Soc. Rev.*, 2014, **43**, 16.

21 L. Antonov and N. Nedeltcheva, *Chem. Soc. Rev.*, 2000, **29**, 217.

22 J. W. Sidman, *Chem. Rev.*, 1958, **58**, 689.

23 See, for example: (*a*) E. Buncel and S. Rajagopal, *Acc. Chem. Res.*, 1990, **23**, 226; (*b*) C. Reichardt, *Chem. Rev.*, 1994, **94**, 2319; (*c*) *Solvents and Solvent Effects in Organic Chemistry*, ed. C. Reichardt and T. Welton, Wiley-VCH, Weinheim, 2011.

24 (*a*) J. Catalán, V. López, P. Pérez, R. Martin-Villamil and J. G. Rodríguez, *Liebigs Ann.*, 1995, 241; (*b*) Also available at: http://www.uam.es/personal_pdi/ciencias/catalan/table.pdf (accessed on December 2015).

25 R. S. Moog, D. D. Kim, J. J. Oberle and S. G. Ostrowski, *J. Phys. Chem.*, 2004, **108**, 9294.

26 Reasonable linear correlations were also obtained with the π^* and π^*_{azo} polarity scales (*r* coefficients = 0.9214-0.9324 for **4f** and 0.9275-0.9583 for **5f**).

27 (*a*) R. Bauernschmitt and R. Ahlrichs, *Chem. Phys. Lett.*, 1996, **256**, 454; (*b*) M. E. Casida, C. Jamorski, K. C. Casida and D. R. Salahub, *J. Chem. Phys.*, 1998, **108**, 4439; (c) R. E. Stratmann, G. E. Scuseria and M. J. Frisch, *J. Chem. Phys.*, 1998, **109**, 8218; (*d*) M. A. L. Marques and E. K. U. Gross, *Ann. Rev. Phys. Chem.*, 2004, **55**, 427; (*e*) A. Bulgac, Y.-L. Luo, P. Magierski, K. J. Roche and Y. Yu, *Science*, 2011, **332**, 1288.

28 (*a*) A. D. Becke, *J. Chem. Phys.*, 1993, **98**, 1372; (*b*) A. D. Becke, *J. Chem. Phys.*, 1993, **98**, 5648.

29 (*a*) C. Lee, R. G. Parr and W. Yang, *Phys. Rev. B*, 1988, **37**, 785; (*b*) P. J. Stephens, J. F. Devlin, C. F. Chabalowski and M. J. Frisch, *J. Phys. Chem.*, 1994, **98**, 11623.

30 M. J. Frisch, G. W. Trucks, H. B. Schlegel, G. E. Scuseria, M. A. Robb, J. R. Cheeseman, J. A. Montgomery Jr., T. Vreven, K. N. Kudin, J. C. Burant, J. M. Millam, S. S. Lyengar, J. Tomasi, V. Barone, B. Mennucci, M. Cossi, G. Scalmini, N. Rega, G. A. Petersson, H. Nakatsuji, M. Hada, M. Ehara, K. Toyota, R. Fukuda, J. Hasegawa, M. Ishida, T. Nakajima, Y. Honda, O. Kitao, H. Nakai, M. Klene, X. Li, J. E. Knox, H. P. Hratchian, J. B. Cross, C. Adamo, J. Jaramillo, R. Gomperts, R. E. Stratmann, O. Yazyev, A. J. Austin, R. Camml, C. Pomelli, J. W. Ochterski, P. Y. Ayala, K. Morokuma, G. A. Voth, P. Salvador, J. J. Dannenberg, V. G. Zakrzewski, S. Dapprich, A. D. Daniels, M. C. Strain, O. Farkas, D. K. Malick, A. D. Rabuck, K. Raghavachari, J. B. Foresman, J. V. Ortiz, Q. Cui, A. G. Baboul, S. Clifford, J. Cioslowski, B. B. Stefanov, G. Liu, A. Liashenko, P. Piskorz, I. Komaromi, R. L. Martin, D. J. Fox, T. Keith, M. A. Al-Laham, C. Y. Peng, A. Nanayakkara, M. Challacombe, P. M. W. Gill, B. Johnson, W. Chen, M. W. Wong, C. Gonzalez and J. A. Pople, *Gaussian 03*, revision C.02, Gaussian Inc., Pittsburgh PA, 2004.

31 W. J. Hehre, L. Radom, P. v. R. Schleyer and J. A. Pople, *Ab Initio Molecular Orbital Theory*, Wiley, New York, 1986.

32 *Chemcraft*, Version 1.7 (Build 382), Bluesnap, Inc., Waltham, Massachusetts, 2013 (http://www.chemcraftprog.com).

33 *CrysAlisPro CCD* & *CrysAlisPro RED,* Oxford Diffraction Ltd., Oxford, UK, 2008.

34 L. J. Farrugia, *J. Appl. Crystallogr.*, 2012, **45**, 849.

35 G. M. Sheldrick, *SHELXL97 - Program for X-Ray Crystal Structure Refinement,* University of Göttingen, Göttingen, Germany, 1997.

36 *International Tables for X-Ray Crystallography, Volume C*, Kluwer Academic Publishers, Dordrecht, The Netherlands, 1992.

37 M. Nardelli, *Comput. Chem.*, 1983, **7**, 95.

38 *DIAMOND - Crystal and Molecular Structure Visualization*, Crystal Impact - Dr. H. Putz & Dr. K. Branderburg, Bonn, Germany (http://crystalimpact.com/diamond).

For Graphical Abstract use only

Novel 1,1-diaryl-substituted butadiene dyes containing 3-(dicyanomethylidene)indan-1-one and 1,3-bis(dicyanomethylidene)indane as groups have been synthetized, and their light absorption and solvatochromic properties evaluated.

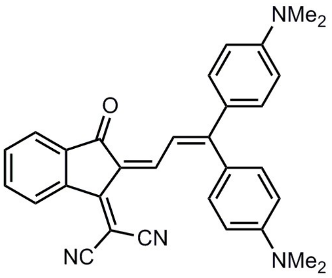

λ_{max} from 633 to 694 nm

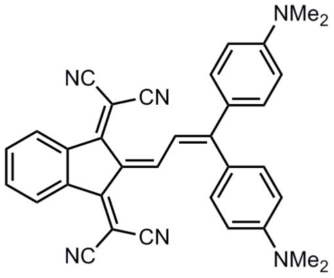

λ_{max} from 669 to 718 nm